Engineering Science and Military Technologies
Volume (8) - Issue (2) - Sep 2024

ISSN: 2357- 0954
DOI:10.21608/EJMTC.2024.250670.1270

Study the performance of turbofan enginesunder the effect of changing chevron nozzle geometry

Original Article

Hany Saad, Khalid Ibrahim, Mahmoud Kamal, Tamer Elnady, Walid Aboelsoud

Department of Mechanical Power Engineering, Faculty of Engineering, Ain Shams University, Cairo, Egypt

Keywords:

Aeroacoustics, chevron nozzle, flow noise, jet noise suppression, turbulent mixing noise, turbofan engine.

Corresponding Author:

Hany Saad, Department of Mechanical Power Engineering, Ain Shams University, Cairo, Egypt, **Tel.:** 01000385638 **Email:** hany.elsayed@eng.asu.edu.eg

Abstract

In this study, the effect of changing the geometry of the chevron nozzle on the performance of turbofan engines is investigated. The study aims to characterize new chevron geometry configurations to investigate how to reduce the jet noise of turbofan engines while achieving minimal impact on engine thrust. To this end, a numerical analysis of the chevron nozzle with different geometries will be performed. The model is validated and compared with experimental and numerical data from the literature. Circular, elliptical, and triangular chevron cutout patterns with different penetration lengths are selected for the jet acoustic characterization of chevron nozzles. These cutouts are applied to both the core nozzle and the fan nozzle, resulting in a double chevron nozzle. The numerical study is performed using a steady 3D density-based k-ε turbulence model. The numerical results are compared with the base nozzle model with no cutout. It was found that best performing geometry in terms of minimizing noise level with gain in thrust compared to the base nozzle model was the circular-shaped Chevron with core diameter to penetration length ratio (penetration ratio) of 5 (DC 5). Furthermore, it was also found that increasing the penetration length will increase the thrust gain of the engine.

1. INTRODUCTION

Aircraft engine performance has become an interesting topic for researchers and scientists. As the volume of air traffic increases the intent to develop HighSpeed Civil Transport (HSCT) aircraft. Moreover, the environmental impact of jet noise is a significant concern for communities who live near airports and in the direct flight path of commercial routes. The potential inclusion of supersonic transports in the future would require enough noise control to meet the same noise regulations as modern subsonic airliners. The aircraft jet noise reduction is a crucial problem in aero-acoustics research due to its negative impact on the environment[1]. Manufacturers of aircraft engines and aircrafts arefacing great challenge of makingpowerful, efficient yet quieter aircrafts. The current study is motivated by the conflicting requirements of these goalsand thusseeks to apply the control of aircraft noise to limit the acoustic level while minimizing the impact on performance[2]. Unfortunately, performance is usually inversely proportionalto acoustics; that is, generally what's good for performance is bad for acoustics. The art is in designing a nozzle that minimizes negative performance impact and maximizes acoustic benefit while meeting the remaining system requirements[3].

The three main sources of acoustic in aircraft are noise from aircraft systems and engine, aerodynamics noise, and mechanical noise[1]. The self-generated noise in the airframe is a factor in the aircraft's overall noise level, but the engine is the main noise source. It is necessary to know the noise sources and their relative importance to understand the problem of engine noise suppression. The significant sources originate in the turbine, the compressor or fan, and the exhaust jet. The basic concept of jet noise generation is due to relative airflow velocity which produces shear stress. The exhaust jet noise is more significant than noise generated by the turbine or the compressor, thereforethe reduction of the noise produced by the exhaust jet has a stronger effect than an equivalent reduction of other mechanical components[4].

Among these noise sources, engine noise contributesthe most in sound pollution of the environment. Although turbofan engines witha high bypassratio have considerable fan noise, most of the engine noise is duethe jet coming out from the exhaust nozzle. In the last few decades,many studies have been carried out to complete understanding of the noise of the jet mechanisms which is still a complicated task[1].

There have been many methods to reduce the noise generated by the jet such as the Nanomaterials, Chevron

nozzle, increasing the bypass ratio in turbofans, extending the engine nacelle, and acoustic lines of the main engine. Chevron nozzle is these nozzles which have corrugated structure at the exhaust section. This corrugatedgeometry is responsible for the smooth mixing ofthe bypass and hot stream or between the outside air and the bypass stream. Therefore, the energy of the turbulence is reduced. The Nanomaterials can absorb the noise within the nozzle due to the high density of the material. In turbofan engines, increasing the bypass ratio is a good option as it reduces the energy of the mainstream by mixing the hot and the cold streams. Adding acoustic lines is another solution for noise reduction;which converts the energy of turbulence into heat. Noise can also be reduced by increasing the size of the engine housing. At this condition, the hot jet will not be directly exposed to the atmosphere but passes through the nacelle first which can absorb the noise by some amount[5].

Jet noise generation in modern jetaircraft is caused by the generated turbulence due to shear layers created at the exhaust. There are two such shear layers generating noise for the separate flow exhaust design which are common in large commercial aircraft; the inner and outer shear layers. The inner shear layer is the layer between core flowand fan flow. The outer shear layer lies between the freestream flow and the secondary (fan flow). At any operating condition,there is a significant shear velocity across one or both shear layers. These shear layers are unstable and lead to vortex generation and turbulence. Robust structures and turbulent eddies generate non-equilibrium pressure fluctuations which are radiated as sound[6] as shown in Figure 1.

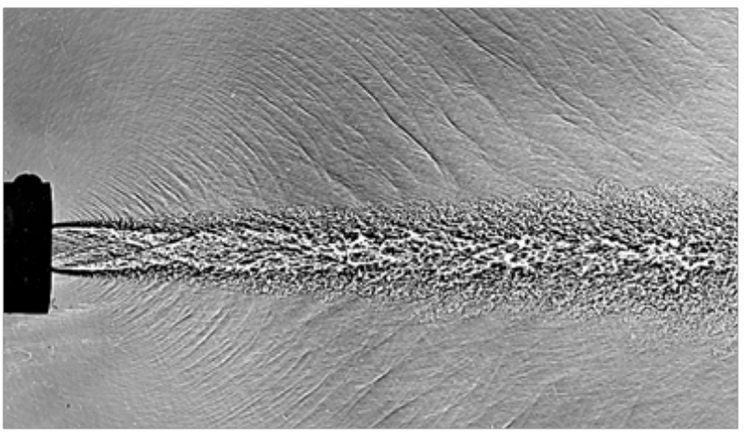

Fig. 1: Shadowgraph of a Mach 2.0 cold jet showing intense Mach wave radiation[7]

Just after the exhaust duct,thegenerated eddies cause high-frequency noise. In downstream of the exhaust jet,however,the larger eddies create low frequency noise. In addition, a regular shock pattern is formed within the exhaust jet core when the exhaust jet velocity exceeds the local speed of sound. Consequently,a discrete (single frequency) tone and selective amplification of the mixing noise will be produced as shown in Figure 2.

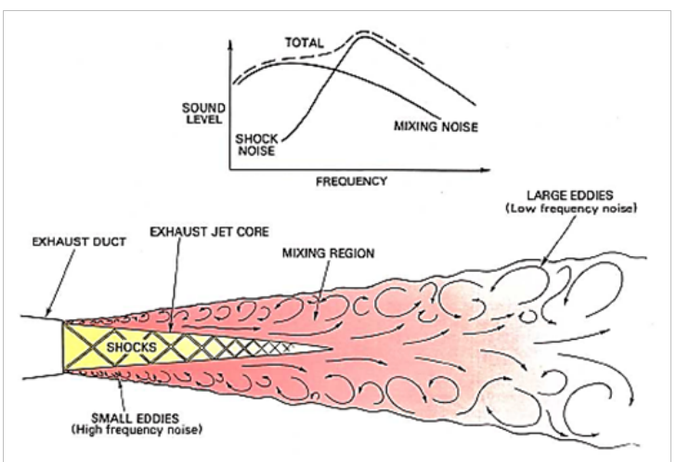

Fig. 2: Exhaust mixing and shock structure[4]

To achieve a reduction in noise level, the rate of mixing betweenthe jet and the surroundings must be accelerated. This occurs if the velocity of the exhaust jet relative to the atmosphere is reduced. The air must be encouraged to mix faster with the surroundingwhich could be achieved by changing the exhaust jet pattern to improve its mixing capability. As described previously, the major source of noise is the exhaust jet on the low by-pass engine and the pure jet engine.This can be reduced by inducing a shorter or rapid mixing region. This will reduce the low frequency of thenoise but may increase the high level of frequency. Luckily though, high frequencies are absorbed quickly in the atmosphere and some of the noise is beyond the audible rangewhich gives the perception of a quieter engine. This can be achieved by increasing the contact area between the atmosphere and the exhaust gas stream by using a propelling nozzle incorporating a corrugated or lobe-type noise suppressor as an example[4].

The University of Cincinnati has an active Aeroacoustics program studying the application of several flow control technologies of typical separate-flow exhaust systems like those found in modern jet engines. Various Chevron geometries are tested and evaluated. Those technologies that show merit are then selected for further testing in collaboration with their industrial partners at GE Aviation and GE Global Research. Though GE Aircraft Engines own test facility, known as Cell 41 the complexity of this facility makes it not a cost-effective option for testing and not particularly feasible for rapidly screening innovative new jet noise reduction concepts. Therefore, it was determined thatthe University of Cincinnati Aero-acoustic Test Facility (UC-ATF)is a less complex facility and the model under test allows quick and easy installation of interchangeable hardware such as different Chevron nozzle models. Although testing at GE allows larger scale and improved fidelity, UC-ATF allows further down the selection path to full-scale engine tests for the best technologies[4,6,8-10].

Due to aircraft noise certification requirements and airport regulations, jet engine noise suppression in the aviation field is required and that is one of the most promising research topics in the field. The effective Perceived Noise decibel (EPNdB) is the unit that is commonly used to express noise annoyance. The pitch as well as the sound pressure (decibel) isconsidered and makes allowance for the duration of an aircraft flyover. The noise level of various jet engine types is shown in Figure 3.

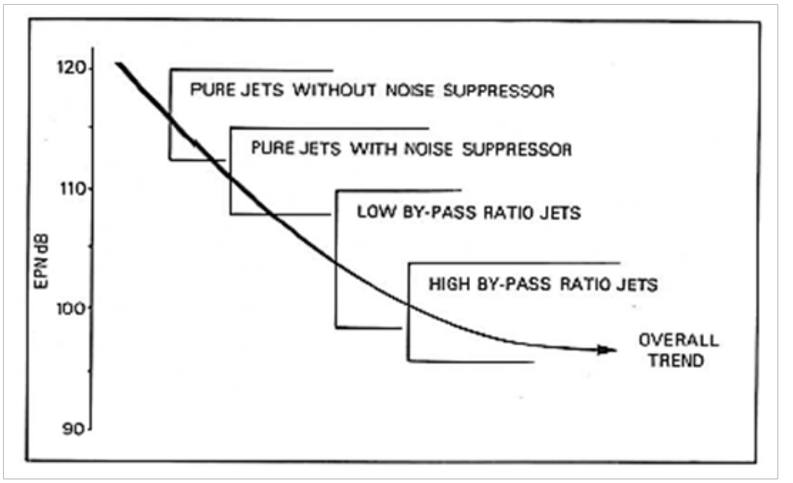

Fig. 3: Comparative noise levels of various engine types[4].

The turbojetwas thestate-of-the-art engine technology in the late 1950s which had a very high level of noise.The majority of which was due to very high jet noise levels. The turbofan was developed over the following decades with the tendency to increase the bypass ratio thus loweringthe noise level. Today turbofan engines typically havea bypass ratioof up to 9, with jet noise remaining the dominant source of aircraft noise, especially at take-off[4].

NASA initiated the Advanced Subsonic Technology Program (AST) in the late 1980s, which focused on the reduction of jet noise for commercial high bypass ratio engines. The High-Speed Civil Transport (HSCT) and the Supersonic Transport (SST) programs are good examples of how difficult the reduction ofjet noise is because these programs were canceled before making it to the product stage.The problem of high jet noise levels and the lack of a technically and economically acceptable means to reduce jet noise were the large factorsfor these cancellations[11,12].

The history of the noise reduction programs is shown in Figure 4. In early 1999, a program to develop an upgrade noise reduction package for the A321 engine was started. The Chevron nozzle was the major element of this upgrade package and it was anticipated to provide a significant amount of noise reduction. The goal was to maximize the reduction of noise using the Chevron in addition to minimizing any negative impacts on the rest of the aircraft/ engine system. This technology was first implemented in an airplane in 2001 and has become part of the production of the exhaust system[3].

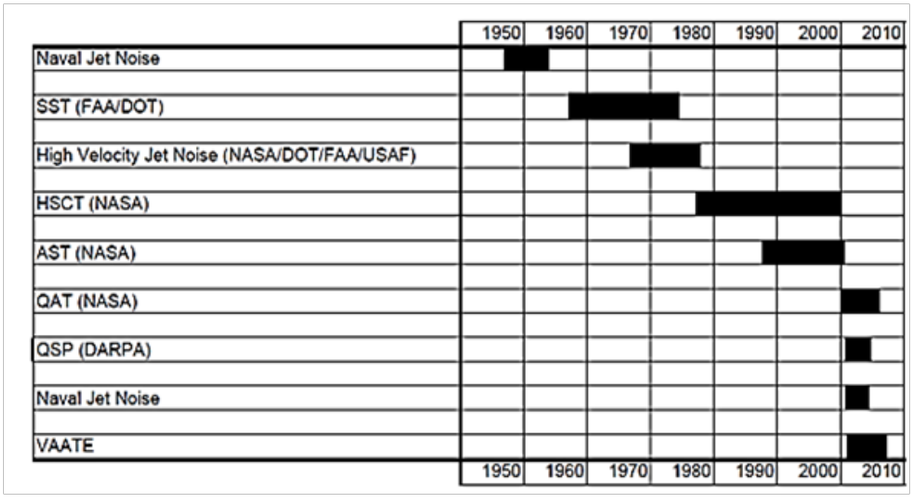

Fig. 4: History of jet noise reduction programs GE Aircraft Engines has been involved in[3].

'Chevron'is defined by Zaman *et al.*[13] as a sawtooth pattern being implemented in modern jet engine nozzles on the trailing edge of exhaust nozzles which significantly helps to reduce the noise from the exhaust jets, as shown in Figure 5

Fig. 5: Chevron nozzle flight test with Honeywell's Falcon 20 test[13].

Earlier experimental studies,with laboratory-scale jets,showed that small protrusions at the nozzle lip, called 'tabs', would suppress noise. By the end of 1990 tab design and geometrywere examined extensively to enhance the mixing in jets. These studies contributed to increasingthe understanding of the flow field mechanisms and suggested techniquesthat might have the potential to reducethe turbulent mixing noise which is dominating jet noise of most aircraft[13].

It was also shown that the reduction of noise in nozzles is of great interest to the aerospace industry, such as the serrated (or Chevron) nozzle[14]. The comprehensive experimental investigations made by Saiyed *et al.*[15, 16] showed that the modification in Chevron of the round nozzle can reduce the peak noise during take-off by 3 dB with less than 0.5 % thrust loss during cruise. Also, the use of Chevrons may lead to about to 2 dB noise increase for high frequencies and large angles to the jet. This therefore leads to the Chevron design optimization problem in which flow and acoustic modeling techniques for jet noise prediction are crucial to achieve maximum reduction in noise level with minimum compromise in engine performance. A numerical study of Chevron jet noisewas carried out by Hao Xia[17]. Hybrid large-eddy type simulation for Chevron nozzle jet flows was performed at Mach 0.9 and Re ~ 105. Many studies were carried out on Chevron nozzles for various applications by many researchers and a new type of Chevron nozzle was installed inside the supersonic ejector-diffuser system as reported by Kong *et al*.[18].

It was also found that the Chevron nozzle is widely used in aircraft engines and aerospace engineering because it has many advantages, such as reducing jet noise, improving the conventional converging-diverging nozzle or converging nozzle, and controlling the infrared signature control[19]. Blaisdell *et al.*[20] also reported that Chevrons improve the performance of conventional nozzles. Thus, chevron nozzles provide the flexibility to control thrust performance and acoustic level[21-31]. Previous studies also reveal that the potential of nozzles for aircraft engines is promising in terms of noise reduction, especially during takeoff. Acoustics studies have shown that the addition of chevrons to jet nozzles reduces sound pressure levels with acceptable performance degradation.

Chevronis not only reducing the jet noise but also broadband shock-associated noise at cruise.The turbulence near the nozzle exit could increase high-frequency noise; however, more understanding of the jet noise is needed[1]. After testing several design concepts,the Chevron nozzle was chosen with various alterationsof the design parameters. Some of these parameters arelength, width, number of Chevrons or cut-outs, aspect ratio, penetration,

sweep angle, shape, relative axial location, azimuthal contouring, etc. Initial design screening was established by using computational fluid dynamics (CFD) analysis to qualitatively do a comparison between the mixing characteristics of the jet plume for different Chevron designs relative to the baseline configuration[3].

Many investigations were carried out by earlier studies to understand the fundamental mechanisms responsible for the influence of various geometric parameters of Chevrons and the acoustic benefit. However, the relationship between the parametersis still not clear. Parameters such as the lobe length,the number of Chevron lobes, and the level of penetration of the Chevrons into the flow have been studied with different flow conditions. Although experiments are essential and give useful data to validateany computation, it is expensive and can supply a relatively limited amount of information.Hence it is preferred to performnumerical modeling to quickly evaluate preliminary designs for noise reduction[1].

Chevron technology can be used to reduce jet noise in aerospace applications. It is extremely difficult to reduce jet noise without negatively impacting engine thrust. The chevron nozzle is unique and has a relatively small impact on performance, weight, and operability[3].

Haukur E. Hafsteinsson, *et al*. studied the mass flow injection in a steady state into a supersonic jet flow using a large eddy simulation with flapping motion and without. particle image velocimetry and acoustic measurements are validated with the results[34].

This study aims to model the chevron nozzle in a turbofan engine using numerical analysis with the finite element method (FEM). The numerical model of the chevron nozzle with different geometries was created and scaled down based on one of the models previously studied at UC-ATF. After achieving dynamic similarity, the model is then validated with experimental and numerical data obtained from UC-ATF. The results of this model allow the proper selection of the chevron nozzle for use in turbofan engines.

2. NUMERICAL MODEL

The finite element method (FEM) is used to model the physics of high velocity compressible fluid flow and to solve for the temperature, velocity, and pressure fields. Acoustic characteristics of jet noise can be evaluated using many parameters such as Strouhal number, turbulent kinetic energy, sound pressure level, … etc. From a computational point of view, it is difficult to treat acoustic physics together with compressible flow physics. The compressible flow governing equations are solved to determine the velocity field. Acoustic characteristics are determined based on the turbulence intensity to evaluate the noise behavior of the jet. COMSOL Multiphysics is used to model the physics of high velocity compressible fluid flow, physics and the results are used to predict the acoustic behavior of various geometries. This captures the dynamics of turbulence, which is significantly related to noise generation. An early study of this problem was presented[8] and a detailed analysis of experimental data was investigated[6, 9].

2.1. Geometry

The three geometries of the chevron nozzles and the base nozzle model studied are shown in Figure 6 and Table 1. The three geometries are defined by the shape type and the ratio of core diameter to penetration length (penetration ratio, Dc/L). This study focuses on the effects of chevron shape and penetration length. The penetration ratio (Dc/L) changed for each shape, as shown in Table 1. The three geometries were tested under the same conditions. In all three cases, the number of chevrons was constant: twelve at the fan nozzle exit and six at the core nozzle exit, as shown in Figure 6.

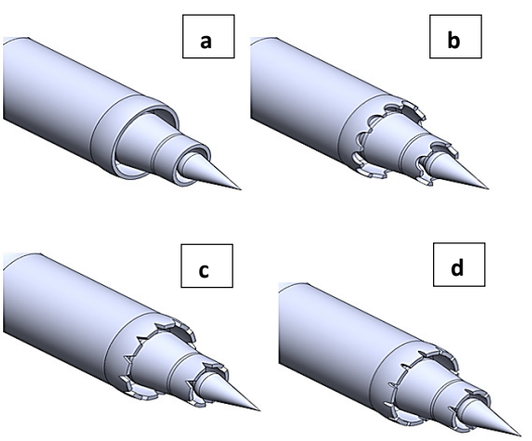

Fig. 6: The 3D models of different configurations of dual Chevron- a) base nozzle model-b) Chevron with circular edge (DC) -c) Chevron with triangle edge (DT) -d) Chevron with ellipseedge (DE)

Table 1: Different Chevron penetration ratios (Dc/L)

CONFIGURATION	Penetration Ratio (DC/L)					
CIRCULAR (DC)	DC 5	DC 10	DC 15	DC 20	DC 30	DC 40
	5	10	15	20	30	40
TRIANGLE (DT)	DT 5	DT 10	DT 15	DT 20	DT 30	DT 40
	5	10	15	20	30	40
ELLIPSE (DE)	DE 5	DE 10	DE 15	DE 20	DE 30	DE 40
	5	10	15	20	30	40

The baseline model tested at the University of Cincinnati Acoustics Test Facility (UC-ATF) is a downscaled model of a typical commercial jet engine (GE CF6-80C2) with separated exhaust flow and mid-bypass. However, in this study, the current model is dynamically similar to the model at UC-ATF with a quarter downscale, as shown in Figure 7.

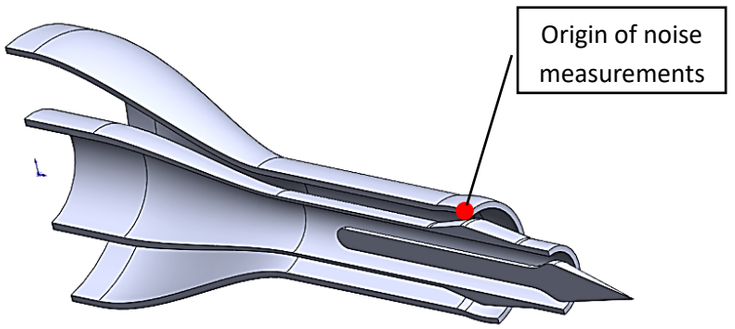

Fig.7: Base nozzle with internal plug (3D) drawing

2.2. Computational Domain

The computational domain is divided into two main domains as shown inFigure 8. The first is the downstream air domain which is selected to be cylindrical due to the symmetry of the nozzle. The dimensions of the air domain downstream such as length and width are selected to cover all the details of the velocity field and its turbulence shear structure, as shown in Figure 8.

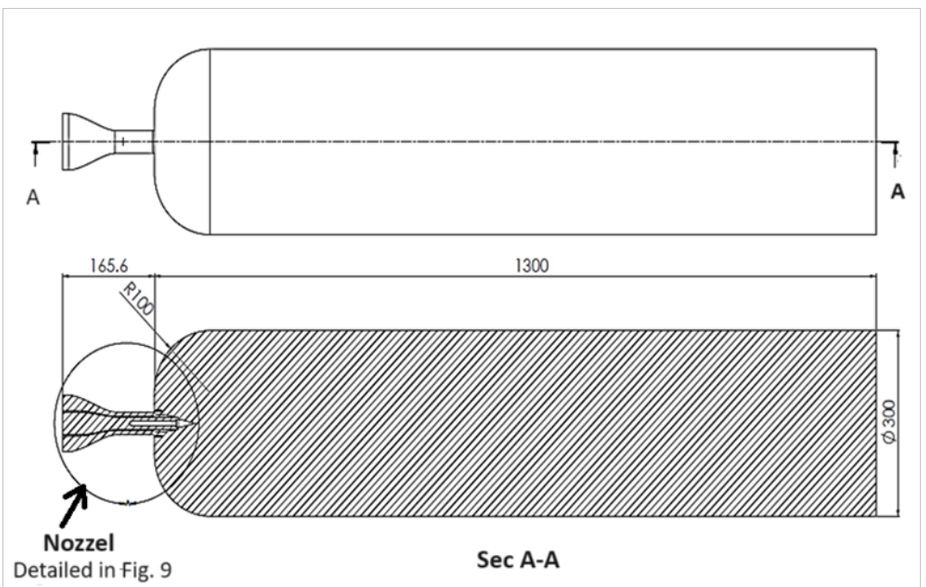

Fig. 8: Computational Domain (2D) - dimensions (mm)

Figure 9 shows a detailed view of the base nozzle model under study.The air domain after the nozzle exit downstream was selected to be cylindrical due to the symmetry of the nozzle. The length and diameter of the air domain downstream were selected to cover all the details in the velocity field and its turbulence shear structure. The length of the air domain downstream is 1300 mm and the diameter is 300 mm.

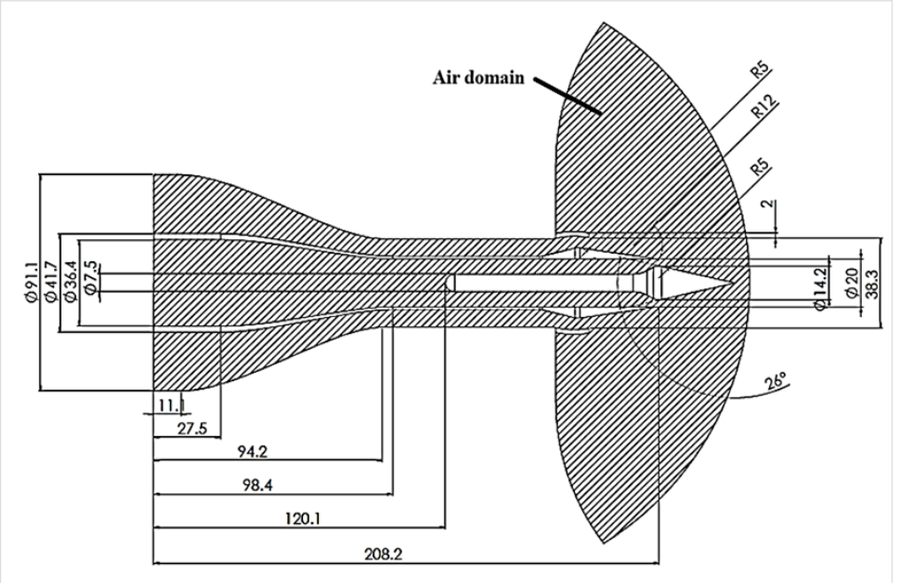

Fig. 9: Base nozzle model (2D) - dimensions (mm)

2.3. Boundary Conditions

Test boundary conditions are shown in Figure 10. To meet medium bypass turbofan engine, the following set of boundary conditions are used:

a) Total temperature and pressure of core flow are 394.3 K and 1.85 atmrespectively at the core inlet.
b) Total temperature and pressure of fan flow are 288.7 K and 1.3195 atmat the fan inlet.
c) Core inlet Mach number of 0.15.
d) Fan inlet Mach number of 0.14.
e) Outlet static pressure of 1 atm.

Fig. 10: Fluid flow domain with inlet and outlet boundaries

2.4. Mesh

As the velocity gradient tensor varies in the computational domain, it was decided to split the domain into two regimes, as shown inFigure 11.The severe shear regime where the core flow and the fan flow exit from the nozzle require intensive computation to capture occurring details. The second regime is the normal shear regime where the velocity gradient tensor can be captured and represented by the numerical model without huge computational effort and cost. This way it was possible to reduce the computational time from 2 days to only 15 hours at most and the number of mesh elements was reduced from roughly ten million to five million with an error in thrust measurement of (0.1%) compared to the mesh with the highest number of elements.Mesh dependency test was performed based on the velocity ratio profile (U/Umax) measured downstream at a distance of 2.5 times the equivalent diameter (Deq = (DFan+DCore)/2) as shown in Figure 12 and Table 2.A mesh dependency test was also carried out based on thrust measurements of the base nozzle model as shown in Figure 13. Thrust is calculated as a “Thrust ratio” which is the ratio of the change in thrust of the selected geometry relative to the base nozzle model. The number of elements in the mesh dependency testvaries from 329,834 elements to 9,750,602 elements as shown in Table 2.

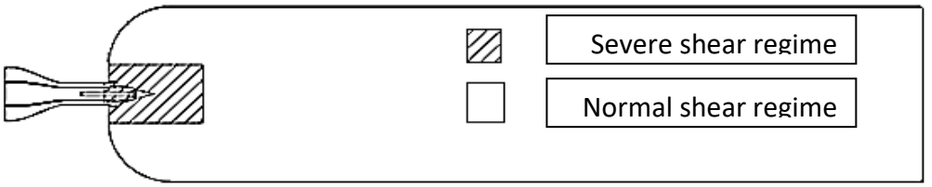

Fig. 11: Domain of Fluid flow after splitting into two mesh sizes

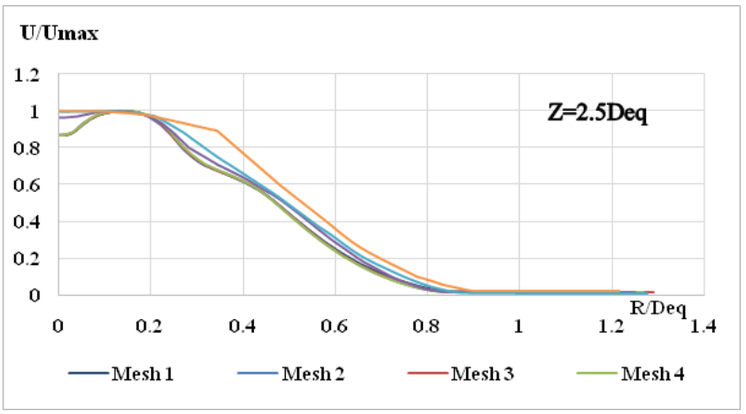

Fig. 12: Mesh dependency test with velocity ratio profile

Table 2: Number of Elements for Each Mesh Size (Mesh dependency test)

MESH	Number of elements (N.O.E)
Mesh 1	9750602
Mesh 2	6217592
Mesh 3	5413938
Mesh 4	5197675
Mesh 5	1155084
Mesh 6	590289
Mesh 7	329834

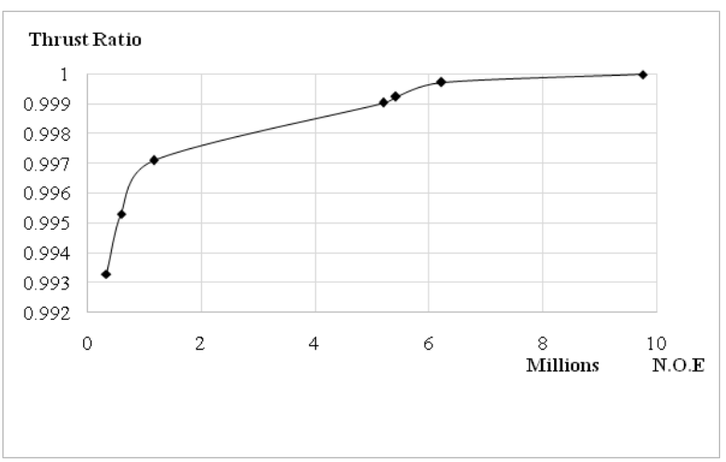

Fig. 13: Base nozzle thrust ratio (Mesh dependency test)

Domain dependency test was also performed which revealed that an air domain downstream of 1300 mm length is enough to achieve zero-shear condition. Based on results from the mesh dependency test and domain dependency test, the discretized computational domain is selected to consist of 5,197,675 elements for all cases under study. The average element quality within the model is 0.7711 at an average growth rate of 1.612.

2.5. Validation

Validation is performed with experimental and numerical results that were conducted by Ephraim Gutmark[6] with atested model of a medium by-pass turbofan engine.The experimental uncertainty provided was ±5 %[6,32,33]. The following set of common boundary conditions is defined:

a) Total temperature and pressure of core flow are 388.7 K and 1.85 atm respectively.
b) Total temperature and pressure of fan flow are 305.37 K and 1.307 atm respectively.
c) Core inlet Mach number of 0.15.
d) Fan inlet Mach number at the inlet of 0.14.

Figure 14 shows a comparison between numerical results of the model under study compared to experimental data[6] in terms of normalized time-average axial velocity profiles along a radial line located downstream ata distance from the fan exit nozzle plane that is 2.5 times the equivalent diameter. There is a very good agreement between the current model and the experimental results[6].

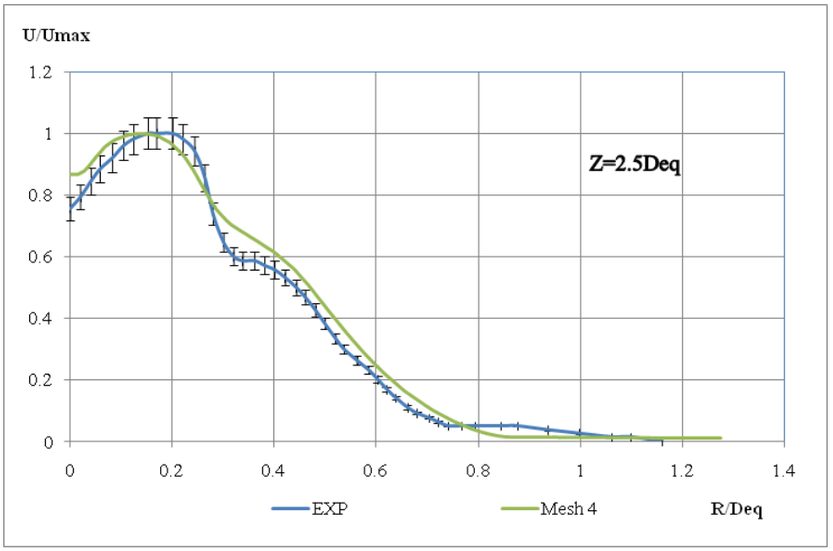

Fig. 14: Radial profiles of time-averaged axial velocity compared to experimental[6]

2.6. Governing Equations

This study was carried out using (FEM). High Mach Number Turbulent Flow, k-ε interface is used to model gas flow at high Reynolds number where the velocity magnitude is comparable to the speed of sound at nozzle exit.A numerical model of the conservation of energy, mass, and momentum is built for Chevron nozzle geometries under studywith steady-state condition. Turbulence effects are modeled using the standard two-equation k-ε model. Flow and heat transfer close to walls are modeled using wall functions. Governing equations are illustrated below, Equations (1-12)[32] while equation (13) is the momentum equation result from the control volume analysis.

Continuity Equation

$$\nabla.(\rho \mathbf{v}) = 0 \tag{1}$$

Momentum Equation

$$\rho(\mathbf{v}.\nabla)\mathbf{v} = \nabla.\left[-p\mathbf{I} + (\mu + \mu_T)\left(\nabla\mathbf{v} + (\nabla\mathbf{v})^T\right) - \frac{2}{3}(\mu + \mu_T)(\nabla.\mathbf{v})\mathbf{I} - \frac{2}{3}\rho K\mathbf{I}\right] + F \tag{2}$$

The Turbulence Modeling Equations:

$$\rho(\mathbf{v}.\nabla)K = \nabla.\left[\left(\mu + \frac{\mu_T}{\sigma_K}\right)\nabla K\right] + P_K - \rho_\epsilon \tag{3}$$

$$\rho(u.\nabla)\epsilon = \nabla.\left[\left(\mu + \frac{\mu_T}{\sigma_K}\right)\nabla\epsilon\right] + C_{e1}\frac{\epsilon}{K}P_K - C_{e2}\rho\frac{\epsilon^2}{K}, \qquad \epsilon = ep, \qquad \mu_T = \rho C_\mu \frac{K^2}{\epsilon} \tag{4}$$

$$P_K = \mu_T \left[\nabla \mathbf{v} : \left(\nabla \mathbf{v} + (\nabla \mathbf{v})^T\right) - \frac{2}{3}(\nabla . \mathbf{v})^2\right] + \frac{2}{3}\rho K \nabla . \mathbf{v} \quad (5)$$

$$K = \frac{2}{3}(UI_T)^2 , \quad \epsilon = C_\mu^{2/3} \frac{K^{2/3}}{L_T} \quad (6)$$

$$I_T = \sqrt{\frac{3}{2}(K)}/U \quad (7)$$

Energy Equation

$$\rho C_P \mathbf{v} . \nabla T = \nabla . (K \nabla T) + Q + Q_{vh} + W_P \quad (8)$$

$$Q_{vh} = \mu\left(\nabla \mathbf{v} + (\nabla \mathbf{v})^T - (2/3)(\nabla . \mathbf{v})\mathbf{I}\right) : \nabla \mathbf{v} \quad (9)$$

$$W_P = \alpha_P T \left(\frac{\partial P_A}{\partial t} + \mathbf{v} . \nabla P_A\right), \text{ where} \frac{\partial P_A}{\partial t} = 0, \alpha_P = -\frac{1}{\rho}\left(\frac{\partial \rho}{\partial T}\right)\Big|_P \quad (10)$$

Sutherland's laws

$$K_s = K_{ref}\left(\frac{T}{T_{K_{ref}}}\right)^{3/2} \frac{T_{K_{ref}+S_K}}{T+S_K} \quad (11)$$

$$\mu = \mu_{ref}\left(\frac{T}{T_{\mu_{ref}}}\right)^{3/2} \frac{T_{\mu_{ref}+S_\mu}}{T+S_\mu} \quad (12)$$

Nozzle Thrust Equation

$$T_F = \left[\left[(\dot{m}_e v_e)_{core} + (\dot{m}_e v_e)_{fan}\right] - \left[(\dot{m}_i v_i)_{core} + (\dot{m}_i v_i)_{fan}\right]\right] + \left[\left[(P_i A_i)_{core} + (P_i A_i)_{fan}\right] - \left[P_e((A_e)_{core} + (A_e)_{fan})\right]\right] \quad (13)$$

3. RESULTS AND DISCUSSION

The present study extends the investigation of the problem and provides numerical analysiswhich leads to proper comparison, thus selecting the best performing Chevron nozzle out of all different shapes. It was decided that the measurement of the thrust, the turbulence intensity, and the peak intensity distance are satisfactory to assess the performance of the nozzle. Turbulence intensity is selected to express the acoustic power which in turn represents noise level. There is a close relationship between turbulence intensity and acoustic power, in other words, they both give the same interpretation of the noise level.

All shapes are tested with penetration ratios of 5, 10, 15, 20, 30 and 40. The acoustic behavior is predicted based on the measured turbulence intensityand its peak distance for primary and secondary shear structures.The turbulence intensity is calculated according to equation 12. The turbulence intensity and its peak distance are calculated on a vertical plane that is symmetric to the computational domain as shown in Figure 8

All measurements are also carried out above the origin. The origin of the measurements is set to be the upper tip at the fan exit section as shown inFigure 7. Measurements of turbulent intensity and its peak distance were performed along a line that starts from the centerline at a corresponding point to the origin of measurements. These lines make an angle with the horizontal, the nozzle directivity angle, at 90o, 110o, 130o, 150o, 170o, and 180o from an origin in the exit section of the fan. They arealso measured along the perpendicular to the centerline of the nozzle(CORE 90).

The thrust is calculated from Equation 13. The mass flow rate is calculated by the integration of air density multiplied by the axial flow velocity at the core and fan

exit sections. Similarly, the rate of change of momentum in the axial direction (thrust) is calculated by the integration of air density multiplied by the axial flow velocity squared at the core and fan exit sections.Thus, a clear idea of the thrust and the noise behavior in each case is obtained and a recommendation for the optimum shape can be made.

The results show turbulence intensity and its peak position for various configurations of base nozzles and Chevron nozzles for all directivity angles. The Chevron model has a good acoustic sound intensity reduction level compared to the base model. Though thrust is reduced in Chevron nozzle configurations compared to normal nozzles, in some cases we need to come up with criteria for selection. Similarly, turbulence intensity is presented. The turbulence intensity peak distance ratio is defined as the distance of the turbulence intensity peak of the base nozzle model minus that of the Chevron nozzle over the distance of the turbulence intensity peak of the base nozzle model. Selection is carried out based on:

1. THRUST

In terms of thrust, the circular chevron performs best among the geometries tested. It is found that the greater the penetration length, the greater the thrust gain. Thus, (DC 5) gives the best thrust gain. Figure 15 and Table 3 show that the thrust of the circular chevron increases by up to 41.3% with increasing penetration length. Further investigation was performed on the geometry (DC 4) geometry to confirm the thrust gain with a further increase in penetration length. The thrust of (DC 4) increased by 69 % compared to the base model. The thrust increase is mainly due to the increase in mass flow rate due to the induction of outside air to the main flow through the chevron openings. Figure 15 also shows that the thrust ratio tends to increase as the penetration ratios under study.

Table 3: Maximum Thrust Ratio

MAX.THRUST RATIO (%)					
CIRCULAR		ELLIPSE		TRIANGLE	
DC 5	41.3	DE 5	24.8	DT 40	10.7

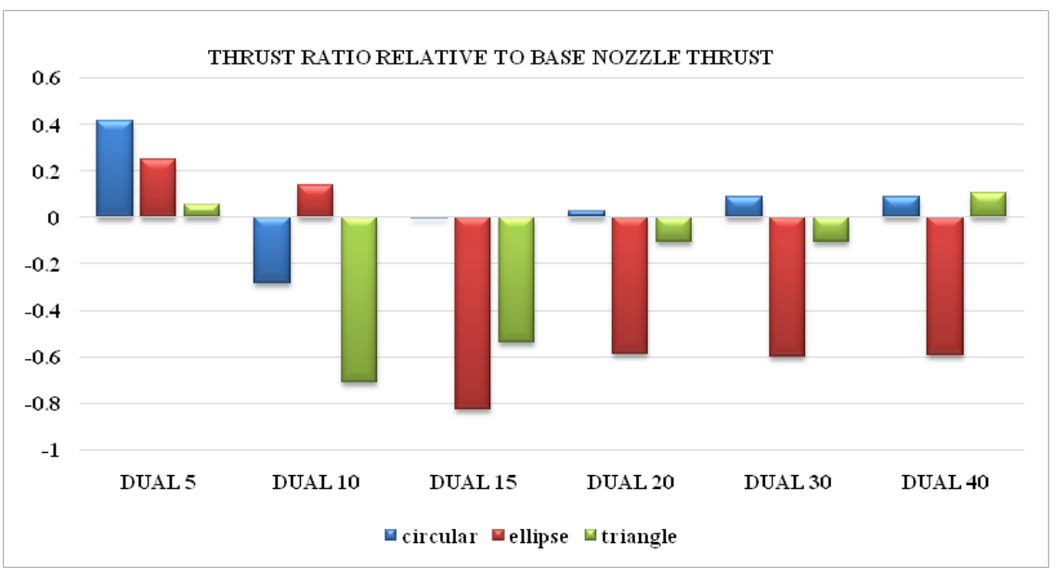

Fig. 15: Ratio of thrust to base nozzle thrust of dual Chevron

2. TURBULENCE INTENSITY PEAK

Turbulence intensity peak value has a great effect on the noise level measurement. The higher the magnitude of the turbulence intensity peak, the higher the noise level. The turbulent intensity peak ratio is defined as the turbulence intensity peak of the Chevron nozzle minus that of the base nozzle model over the turbulence intensity peak of the base nozzle model. Figure 16shows the variation of the turbulence intensity peak ratio with different penetration ratios of each geometry at all directivity angles. The Triangle Chevron (DT 5) and circular Chevron (DC 15) give the maximum reduction of noise level among tested geometries as shown in Table 4.In addition to the six chosen directivity angles, the peak

intensity ratio is measured from the centerline at the same vertical plane of the origin (core 90). These measurements enable to account for the downstream low-frequency noise as well as the high-frequency noise level at the nozzle exit because it is simply a measurement along the centerline

Table 4: Best reduction ratio of Intensity Peak

SHAPE	CIRCULAR		ELLIPSE		TRIANGLE	
90	DC 40	-30.3	DE 15	-33	DT 40	-29.9
110	DC 15	-37	DE 15	-34.1	DT 5	-38.4
130	DC 15	-36	DE 15	-29.3	DT 5	-34.1
150	DC 15	-45.7	DE 15	-36.5	DT 5	-46.2
170	DC 30	-32.3	DE 40	-36.7	DT 40	-44.9
180	DC 5	-10.6	DE 15	-8.5	DT 5	-9.4
Core 90	DC 15	-68.4	DE 15	-75.6	DT 10	-69.5

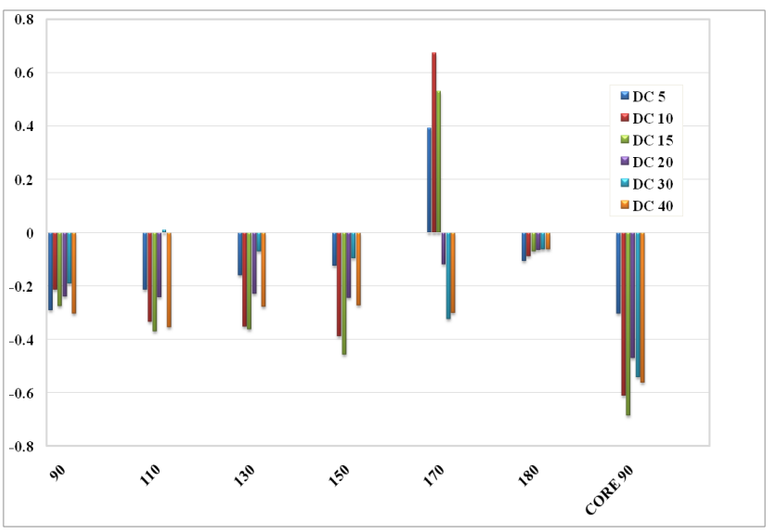

Fig. 16a: Turbulence Intensity Peak Ration -DC

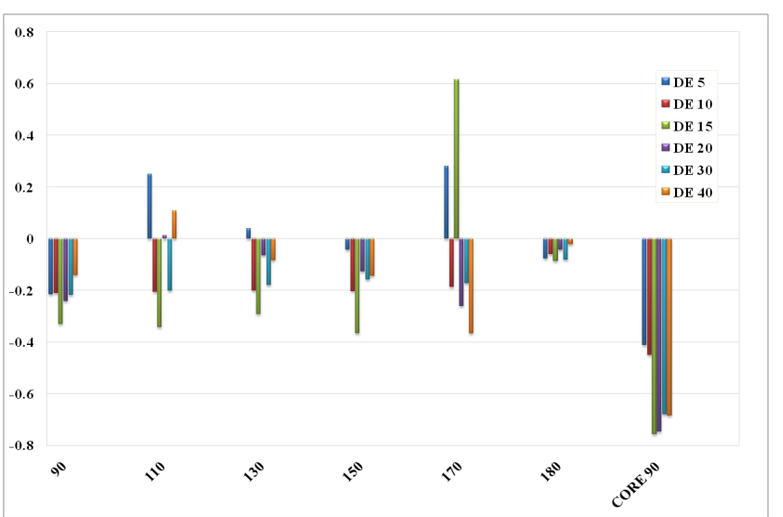

Fig. 16b: Turbulence Intensity Peak Ration -DE

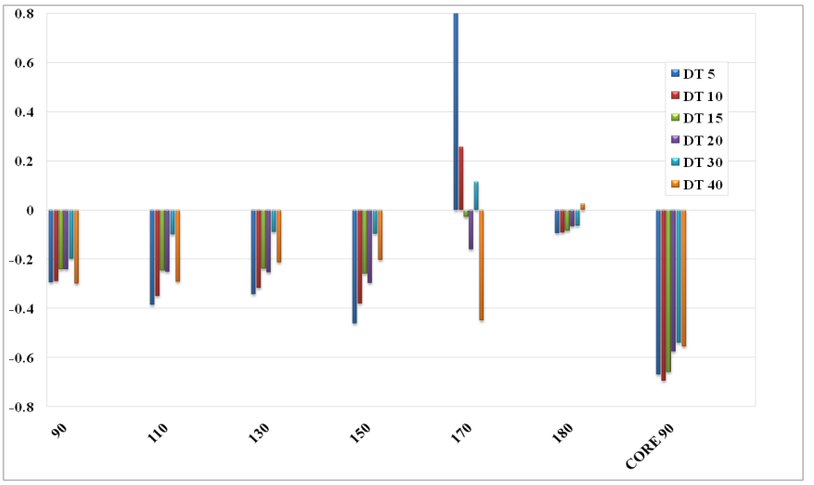

Fig. 16c: Turbulence Intensity Peak Ration -DT

Fig. 16: Turbulence intensity ratio of dual Chevron with different geometry(DC, DE, and DT)

3. TURBULENCE INTENSITY PEAK DISTANCE

Intensity peak distance shift has a great effect on the sound travel distance from the noise source. The more the peak of the sound's travel distance shifts downstream, the greater the noise reduction is anticipated. Figure 17and Table 5 show that a circular Chevron is the best shape in terms of how far the position of the turbulent intensity peak is from the nozzle exit.

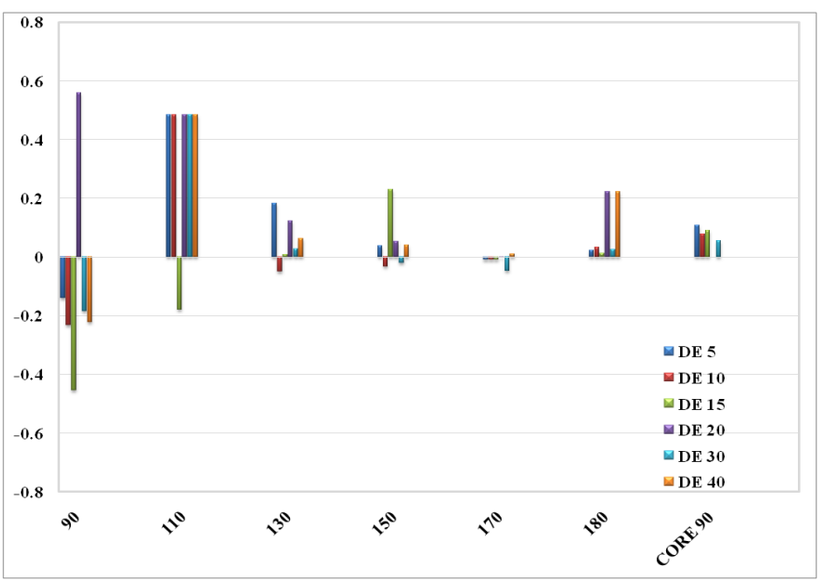

Fig. 17a: Turbulence intensity peak distance ratio - DE

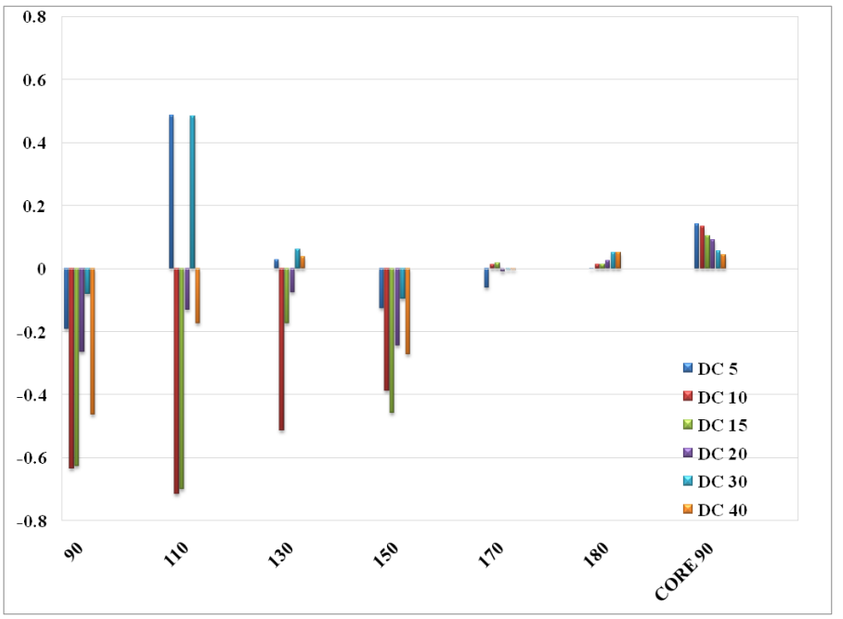

Fig. 17b: Turbulence intensity peak distance ratio - DC

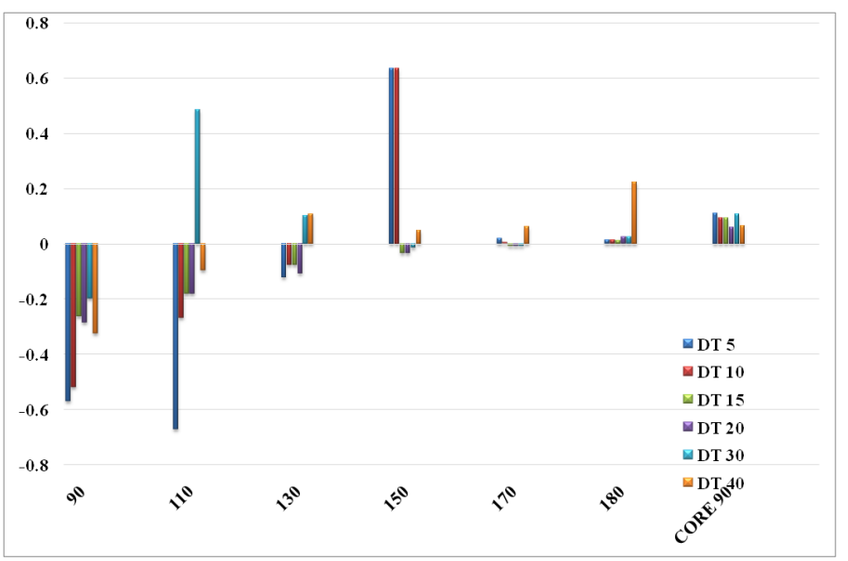

Fig. 17c: Turbulence intensity peak distance ratio - DT

Table 5: Minimum Intensity Peak Distance Ratio

SHAPE	CIRCULAR		ELLIPSE		TRIANGLE	
90	DC 10	-63.3	DE 15	-45.3	DT 5	-56.9
110	DC 10	-71.5	DE 15	-18	DT 5	-67
130	DC 10	-51.4	DE 10	-4.9	DT 5	-12.1
150	DC 15	-45.7	DE 10	-3.3	DT 15	-3.3
170	DC 5	-6.1	DE 30	-4.8	DT 15	-0.87
180	DC 5	0.15	DE 15	1.3	DT 15	1.3
Core 90	DC 40	4.4	DE 30	5.5	DT 40	6

4. TURBULENCE INTENSITY PEAK AND THRUST COMBINED

It is required to come up with a selection criterion for the best geometry that considers the maximum thrust gain as well as the maximum reduction of noise indicators, turbulence intensity peak, and turbulence intensity peak distance. This criterion must include an assessment of the thrust ratio relative to the turbulence intensity peak ratio and turbulence intensity peak distance ratio, respectively. As a result, combined Gain Factor 1 (CGF1) is defined as the difference between the thrust ratio and the turbulent intensity peak ratio. It is also required to eliminate the cases in which negative CGF1 is achieved because that means this Chevron nozzle geometry decreases thrust and increases noise level. Table 6 shows CGF1 for all tested geometries at different directivity angles and different penetration ratios. After applying the elimination process to the cases with degradation in performance, fifty-one cases out of one hundred and twenty-six were excluded from the selection criteria. The maximum CGF1 is achieved with a circular Chevron at five directivity angles out of seven. A penetration ratio of 5 (Dual 5) gives the maximum CGF1 in fourteen cases out of twenty-one (three different shapes at seven directivity angles). In general, circular Chevrons that have the maximum penetration length (DC 5) and minimum penetration ratio outperform elliptical and triangular geometries for the directivity angles under study. This is attributed to the achieved gain in thrust and reduction in turbulent intensity, which together will give the maximum benefit in performance.

Table 6: Combined Gain Factor 1 (CGF1)

Directivity Angle	SHAPE	DUAL 5	DUAL 10	DUAL 15	DUAL 20	DUAL 30	DUAL 40
	CIRCULAR	0.703	Exclude	0.274	0.265	0.279	0.391
90	ELLIPSE	0.463	0.348	Exclude	Exclude	Exclude	Exclude
	TRIANGLE	0.349	Exclude	Exclude	0.131	0.088	0.405
	CIRCULAR	0.627	0.053	0.369	0.267	0.079	0.441
110	ELLIPSE	Exclude	0.344	Exclude	Exclude	Exclude	Exclude
	TRIANGLE	0.440	Exclude	Exclude	0.142	Exclude	0.397
	CIRCULAR	0.572	0.071	0.360	0.256	0.160	0.365
130	ELLIPSE	0.209	0.338	Exclude	Exclude	Exclude	Exclude
	TRIANGLE	0.397	Exclude	Exclude	0.145	Exclude	0.320
	CIRCULAR	0.537	0.106	0.456	0.270	0.183	0.360
150	ELLIPSE	0.290	0.340	Exclude	Exclude	Exclude	Exclude
	TRIANGLE	0.518	Exclude	Exclude	0.188	Exclude	0.310
	CIRCULAR	0.021	Exclude	Exclude	0.146	0.412	0.388
170	ELLIPSE	Exclude	0.323	Exclude	Exclude	Exclude	Exclude
	TRIANGLE	Exclude	Exclude	Exclude	0.051	Exclude	0.556
	CIRCULAR	0.518	Exclude	0.069	0.090	0.150	0.149
180	ELLIPSE	0.325	0.198	Exclude	Exclude	Exclude	Exclude
	TRIANGLE	0.150	Exclude	Exclude	Exclude	Exclude	0.081
	CIRCULAR	0.717	0.330	0.683	0.497	0.631	0.650
CORE 90	ELLIPSE	0.659	0.588	Exclude	0.155	0.082	0.092
	TRIANGLE	0.725	Exclude	0.122	0.468	0.430	0.660

5. TURBULENCE INTENSITY PEAK DISTANCE AND THRUST COMBINED

A second criterion would be the assessment of the thrust gain relative to the reduction in turbulence intensity peak distance ratio. Therefore,combined Gain Factor 2 (CGF2) is defined as the difference between the thrust ratio and the turbulent intensity peak distance ratio. Following the same elimination process for the cases that have negative CGF2,which enables to narrow down the best geometries to choose from. Table 7 shows CGF2 for all tested geometries at different directivity angles and different penetration ratios. Sixty-eight cases, out of one hundred and twenty-six, were excluded from the selection criteria. The maximum CGF2 is achieved with circular Chevron at five directivity angles out of seven. A penetration ratio of 5 (Dual 5) gives the maximum CGF2 in fourteen cases out of twenty-one (three different shapes at seven directivity angles). Results are consistent with those of CGF1. Although the turbulence intensity peak distance could have a smaller influence on the noise level than the turbulence intensity peak itself, the consistent results give acertain degree of confidence in the final decision.

Table 7: Combined Gain Factor 2 (CGF2)

Directivity Angle	SHAPE	DUAL 5	DUAL 10	DUAL 15	DUAL 20	DUAL 30	DUAL 40
	CIRCULAR	0.605	0.352	0.624	0.289	0.168	0.551
90	ELLIPSE	0.386	0.370	Exclude	Exclude	Exclude	Exclude
	TRIANGLE	0.625	Exclude	Exclude	0.176	0.088	0.432
	CIRCULAR	Exclude	0.433	0.699	0.158	Exclude	0.262
110	ELLIPSE	Exclude	Exclude	Exclude	Exclude	Exclude	Exclude
	TRIANGLE	0.726	Exclude	Exclude	0.070	Exclude	0.201
	CIRCULAR	0.386	0.232	0.172	0.100	0.028	0.051
130	ELLIPSE	0.065	0.187	Exclude	Exclude	Exclude	Exclude
	TRIANGLE	0.177	Exclude	Exclude	Exclude	Exclude	Exclude
	CIRCULAR	0.537	0.106	0.456	0.270	0.183	0.360
150	ELLIPSE	0.210	0.171	Exclude	Exclude	Exclude	Exclude
	TRIANGLE	Exclude	Exclude	Exclude	Exclude	Exclude	0.058
	CIRCULAR	0.474	Exclude	Exclude	0.035	0.092	0.091
170	ELLIPSE	0.257	0.147	Exclude	Exclude	Exclude	Exclude
	TRIANGLE	0.036	Exclude	Exclude	Exclude	Exclude	0.045
	CIRCULAR	0.411	Exclude	Exclude	0.001	0.038	0.037
180	ELLIPSE	0.226	0.104	Exclude	Exclude	Exclude	Exclude
	TRIANGLE	0.042	Exclude	Exclude	Exclude	Exclude	Exclude
	CIRCULAR	0.272	Exclude	Exclude	Exclude	0.032	0.044
CORE 90	ELLIPSE	0.139	0.061	Exclude	Exclude	Exclude	Exclude
	TRIANGLE	Exclude	Exclude	Exclude	Exclude	Exclude	0.041

4. CONCLUSIONS

This study aimed to analyze the performance of the circular, elliptical, and triangular shapes of the Chevron nozzle in terms of the change in thrust as well as the change in noise level. The noise level was assessed by the turbulence intensity peak and its distance. The conclusion of the study can be summarized as follows:

• Circular Chevron with a penetration ratio of 5 (DC5) achieveda thrust gain of 41.3%. Further investigation for penetration ratio of 4 (DC4) revealed a 69% gain in thrust.

• Nosie level is assessed based on the turbulent intensity peak and its distance. Results show that a reduction in noise level can be achieved with a longer penetration length or a smaller penetration ratio. A maximum reduction in turbulent intensity of 75.6% is achieved by DE 15. The longest shift of the intensity peak relative to the base nozzle model is 71.5% downstream for DC10.

• Selection criteria are generated to combine the assessments of thrust gain and reduction in noise level, CGF1 and CGF2. The circular chevron at the smallest penetration ratio (DC5) outperforms other geometries in five out of the seven directivity angles under study.

• This study aims to show the effect of the Chevron nozzle on thrust, turbulent intensity peak, and its corresponding distance. Other factors related to the mechanical characteristics of the material must be considered when a selection is made.

• NOMENCLATURE

Symbol - Definition	Value	Unit
R_s - Specific gas constant	287	J/kg.K
C_p - Heat capacity at constant pressure	1005	J/kg.K
γ- Ratio of specific heats	1.4	1
Ce1	1.44	
Ce2	1.92	
Cμ - *k–ε* model parameter	0.09	
σK	1	
σ_e	1.3	
k_v	0.41	
B	5.2	
K_s – Thermal Conductivity		W/m/K
K_{ref}– Conductivity at Reference Temperature	0.0241	W/m/K
$T_{K,ref}$ - Reference Temperature	273	K
S_k– Sutherland Constant	194	K
μ_{ref} – Dynamic Viscosity at Reference Temperature	1.716E-5	Pa.s
$T_{\mu,ref}$– Reference Temperature	273	K
S_μ – Sutherland Constant	111	K
ρ - Fluid Density		kg/m3
v - Velocity Field		m/s
P - Pressure		N/m2
I –Identity Tensor		
c_p - average specific heat of air at constant pressure		(J/kg K)
K – Turbulent Kinetic Energy		m2/s2
ϵ- Turbulent Dissipation Rate		m2/s3
Q_{vh}- Viscous Dissipation		W/m3
Q - Viscous Heating		W/m3
W_p – Pressure Work		Pa/s
T – Temperature		K
α_p - Isobaric compressibility coefficient		K -1
P_k - Turbulent kinetic energy source term		W/m3
I_T – Turbulence Intensity		1
U - mean flow velocity		m/s
L_T - Turbulence or Eddy Length Scale		m
P_{ac} – acoustic power		W
A_s – area of a surface that wholly encompasses the acoustic source		m2
P_0- acoustic power reference	10^{-12}	W
L_p – acoustic power level		dB
T_f – thrust force		N
$\dot{m}_e$- mass flow rate at core/fan exit		Kg/s
$\dot{m}_i$- mass flow rate at core/fan inlet		Kg/s
A_e –core/fan flow exit area		m2
A_i – core/fan flow inlet area		m2
P_i – inlet pressure core/fan flow		pa

P_e – exit pressure	pa
Dc/L - penetration ratio	
DC -Chevron with circular edge	
DT - Chevron with triangle edge	
DE - Chevron with ellipse edge	
U/Umax- The velocity ratio profile measured downstream at a distance of 2.5 times the equivalent diameter	
Z- Radial distance located downstream at a distance from the fan exit nozzle plane	m
CGF- Combined Gain Factor (the thrust gain relative to the reduction in turbulence intensity peak distance ratio)	

5. REFERENCES

[1] Kanmaniraja, R., *et al.*, 3D Numerical Studies on Jets Acoustic Characteristics of Chevron Nozzles for Aerospace Applications. World Academy of Science, Engineering and Technology, International Journal of Mechanical, Aerospace, Industrial, Mechatronic and Manufacturing Engineering, 2014. 8 (9): p. 15251531-.

[2] Peart, N.A. Flyover-noise measurement and prediction. in Aeroacoustics of Flight Vehicles: Theory and Practice. Volume 2: Noise Control. 1991.

[3] Martens, S., JET NOISE REDUCTION TECHNOLOGY DEVELOPMENT AT GE AIRCRAFT ENGINES. 2002.

[4] Rolls-Royce plc. The jet engine. Derby: The Technical Publications Department. ISBN 09021211996 .235-.

[5] Shriwas, S., *et al.*, Reduction of Jet Noise in the Aircraft Nozzle. International Journal of Research in Aeronautical and Mechanical Engineering ISSN (ONLINE), 2015: p. 23213051-.

[6] Rask, O., *et al.*, Jet Aircraft Propulsion Noise Reduction Research at University of Cincinnati. AIAA Paper, AIAA, 2007. 5631: p. 16.

[7] Christopher K. W. Tam. "Mach Wave Radiation from High-Speed Jets", AIAA Journal, Vol. 47, No. 10, pp. 24402009 .2448-.

[8] CALLENDER, W.B., An Investigation of Innovative Technologies for Reduction of Jet Noise in Medium and High Bypass Ratio Turbofan Engines, University of Cincinnati. 2004.

[9] Callender, B., E. Gutmark, and R. Dimicco. The design and validation of a coaxial nozzle acoustic test facility. in 40th AIAA Aerospace Sciences Meeting & Exhibit. 2002.

[10] Saiyed, N.H., K.L. Mikkelsen, and J.E. Bridges, Acoustics and thrust of separate-flow exhaust nozzles with mixing devices for high-bypass-ratio engines. AIAA paper, 2000. 1961(5).

[11] Lighthill, M.J., "On Sound Generated Aerodynamically. I. General Theory," Proceedings of the Royal Society of London, Series A, Volume 211, Issue 1107, pp 5641952 ,587-.

[12] Janardan, B., *et al.*, AST critical propulsion and noise reduction technologies for future commercial subsonic engines: separate-flow exhaust system noise reduction concept evaluation. 2000.

[13] K.B.M.Q. Zaman, J.E. Bridges and D.L. Huff, "Evolution from 'Tabs' to 'Chevron Technology' – a Review," Proceedings of the 13th Asian Congress of Fluid Mechanics, Dhaka, Bangladesh. 1721- December 2010.

[14] Bridges, J., Brown, C. A., "Parametric testing of chevrons on single flow hot jets", AIAA-20042824-; NASA/TM 20042004 ,213107-.

[15] Saiyed, N., "Separate flow nozzle test status meeting", NASA/TM 2000- 210524.

[16] Saiyed, N. Mikkelsen K.L. and Bridges, J., Acoustics and thrust of separate-flow exhaust nozzles with mixing devices for high-bypass-ratio engines, NASA/TM 20002000 .209948-.

[17] Hao Xia, Numerical study of chevron jet noise using parallel flow solver. Science Direct Procedia Engineering 61 (2013) 40 – 47.

[18] Fan Shi Kong, Heuy Dong Kim, Yingzi Jin and Toshiaki Setoguchi, "Application of Chevron nozzle to a supersonic ejector–diffuser system," 5th BSME International Conference on Thermal Engineering, Procedia Engineering 56 (2013) 193 – 200.

[19] Khalid, S., Sokhey, J., Chakka, P., and Pierluissi, A., "Ejector/ Engine/Nacelle Integration for Increased Thrust minus Drag," 46th AIAA/ASME/SAE/ASEE Joint Propulsion Conference and Exhibit, Nashville, TN, USA, AIAA-20106501-, June 2010.

[20] Gregory A. Blaisdell, Anastasios S. Lyrintzis and John P. Sullivan, "Preliminary Design and Computational Analysis of an Ejector Nozzle withChevrons" 49th AIAA Aerospace Sciences Meeting including the New Horizons Forum and Aerospace Exposition, Florida, 2011.

[21] Crow, S.C., Champagne, F.H., "Orderly Structure in Jet Turbulence," Journal of Fluid Mechanics, Vol 48, Part 3, pp 547- 591, 1971.

[22] Brown, G.L., Roshko, A., "On Density Effects and Large Structure in Turbulent Mixing Layers," Journal of Fluid Mechanics, Vol 64, Part 4, pp 7751974 ,816-.

[23] Tam, C.K.W., Golebiowski, M., & Seiner, J.M., "On the Two Components of Turbulent Mixing Noise from Supersonic Jets," AIAA 961996 ,1716-.

[24] Kanmaniraja, R., *et al.*, 3D Numerical Studies on Jets Acoustic Characteristics of Chevron Nozzles for Aerospace Applications. World Academy of Science, Engineering and Technology, International Journal of Mechanical, Aerospace, Industrial, Mechatronic and Manufacturing Engineering, 2014. 8(9): p. 15251531-.

[25] Karabasov, S., Understanding jet noise. Philosophical Transactions of the Royal Society of London A: Mathematical, Physical and Engineering Sciences, 2010. 368(1924): p. 35933608-.

[26] Ffowcs-Williams, "Aeroacoustics", Annual Review of Fluid Mechanics, 9: 447- 468. 1977.

[27] Crow S.C., Champagne, F.H., "Orderly Structure in Jet Turbulence", Journal of Fluid Mechanics Vol 48, Part 3, pp. 547- 591, 1971.

[28] Brown, G.L., Roshko, A,"On Density Effects and Large Structure in Turbulent Mixing Layers", Journal of Fluid Mechanics, Vol 64, Part 4, pp. 7751974 ,816-.

[29] Lilley, G.M., "Jet Noise Classical Theory and Experiment". In "Aeroacoustics of Flight Vehicles", ed. H.H. Hubbard, Vol. 1, pp. 211-289, Acoustical Society of America, 1995.

[30] Shriwas, S., *et al.*, Reduction of Jet Noise in the Aircraft Nozzle. International Journal of Research in Aeronautical and Mechanical Engineering ISSN (ONLINE), 2015: p. 23213051-.

[31] Lighthill, M.J., "On Sound Generated Aerodynamically. II. Turbulence as a source of sound," Proceedings of the Royal Society of London, Series A, Volume 222, Issue 1148, pp 11954 ,32-.

[32] Markus Raffe, *et al.* "PIV Uncertainty and Measurement Accuracy" Particle Image Velocimetry, 2018, pp 203–241.

[33] Andrea Sciacchitano, and Bernhard Wieneke "PIV uncertainty propagation" Measurement Science and Technology, 2016, Volume 27, number 6.

[34] Haukur E. Hafsteinsson, *et al.* "Noise Control of Supersonic Jet with Steady and Flapping Fluidic Injection" AIAA, American Institute of Aeronautics and Astronautics, 2015, Volume 53, Number 11.